International Journal of Scientific Research & Engineering Trends
Volume 4, Issue 5, Sept-Oct-2018, ISSN (Online): 2395-566X

Controller Analysis of Reaction Wheel System for Counter Torque

Ye Min Htay
Dept of Space Systems Engineering
Myanmar Aerospace Engineering University
Meiktila, Mandalay, Myanmar
www.yeminhtay.4@gmail.com

Thu Thu Aung
Dept of Space Systems Engineering
Myanmar Aerospace Engineering University
Meiktila, Mandalay, Myanmar
thuthumdy@gmail.com

Abstract -**This work addresses the reaction wheel system (RWS) for a Nano satellite and simulator which shows the function of it. The object is to design flywheels that counteract the disturbance torques experienced by satellite in the harsh space environment and to stabilize the platform of simulator. The performance of reaction wheels is analyzed to achieve the stable for system. The satellite and simulator utilizes three reaction wheels as actuators. The controller is designed to change the rotational speed of reaction wheels to adjust the satellite and simulator in the desired position. The mathematical model of reaction wheel system using angular kinetic equation is developed. Control theory is then applied for a required response that deals with both non linarites in equations and disturbance sources. Simulation of closed loop system shows that all desired specification of closed loop (rising time, settling time and steady state error) are robustly satisfied.**

Keywords – **reaction wheel system, satellite, simulator, space environment, performance, controller**

I. INTRODUCTION

The use of satellites for scientific, commercial and military purposes have been rising year after year. Over the past years, there has been a huge investment in miniaturizing the space technology and this has given origin to a new kind of satellites, Nano satellites. These satellites are in a range between 1 kg to 10 kg and have become an increasingly popular alternative over the traditional bulkier satellites [1]. One reason for miniaturing satellites is to reduce the cost, i.e., heaviersatellites require larger rockets with greater thrust.Thesmall satellites require more precise attitude determination system. Therefore, the reaction wheel system is crucial role for Nano satellite [2,8,9].

The spacecraft is made of two systems: bus and payload. The bus includes the structure subsystem, thermal subsystem, propulsion subsystem, power subsystem, data handling and command subsystem, antenna subsystem and attitude determination and control subsystem. These subsystems serve the payload to work completely under the harsh space environment [3].

Among of them, Attitude determination and control subsystem is broken down to attitude determination and attitude control.Attitude determination is the process of computing the orientation of the spacecraft relative to either an inertial reference or some object of interest, such as the Earth. This typically involves several types of sensor on each spacecraft and sophisticated data processing procedures and spacecraft hardware to determine its position and orientation. Attitude control is the process of orienting the spacecraft in a specified, predetermined direction. It consists of two areas – attitude stabilization, which is the process of maintaining an existing orientation, and attitude maneuver control, which is the process of controlling the reorientation of spacecraft from one attitude to another.

Reaction wheel system, magnetorquer, control moment gyro (CMG), Jet thruster are used for attitude stabilization and maneuvering [10].

The use of a reaction wheel as an actuator in satellite control has gained popularity lately. Reaction wheels are a combination of a motor and a flywheel and rely on the conservation of spacecraft angular momentum that means, if a reaction wheel accelerates in one direction, the satellite will accelerate in the opposite direction. Reaction wheels are capable of delivering torques that are both larger and more accurate and the delivered torque vector is not limited by external factors. Their limitation is that they have a maximum rotation speed and can therefore become saturated.The combination with magnetorquers is an effective one, because magnetorquers can be employed to desaturate reaction wheels when needed.RWS produces maximum torque from 0.01 to 2.0N-m, maximum angular momentum from 2 to 250 N-m-s by using maximum rotation speeds from 1,000 to 30 ,000 rpm [12].

The performance of the RWS is quantified by the maximum angular momentum, maximum output torque, electrical power, and the level of Nano vibrations produced by the wheels. Increasing angular momentum, maximum output torque, maneuvering time required, vibration from the rotation of wheels, and controller designed is focused in this paper.The structure of paper is organized as follows. Section II describes the mission

designation of Nano satellite. Section III presents the environmental disturbance experienced by Nano satellite.

The flywheel design for Nano satellite and simulator, choosing platform selection is described in section IV. Internal disturbance of reaction wheels is discussed in section 5. System modelling of system is described in section 6 and the controller design and simulation resulted in section 7.

II. MISSION DESIGNATION

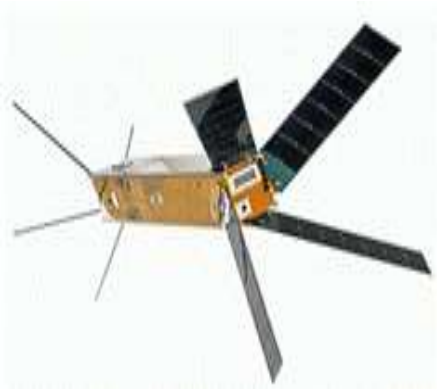

Fig. 1 Nano satellite [12].

The first step for engineering process is defining the mission objective and constraint. The mission objective is to build. Satellite for education service in the poor country and technology demonstration of reaction wheel system. Mission designer manages effectively between time and cost. Nano satellite is selected as shown in Fig. 1 and elliptical orbit in the low regime is used for mission.

To meet the mission objective, orbital parameters and the geometry of satellite is selected as described in Table 1.From the mission data of satellite, the principal moment of inetia in each axis is determined as [11]

$$I = \frac{1}{12} m(a^2+b^2) \quad (1)$$

Here, I is mass moment of inertia for each axis, m is mass of satellite, a and b is the length and width of perpendicular axis. The moment of inertia of individual axis is presented in Table 2.
The physical parameter of satellite is essential for deriving the kinetic and kinematic model in the system.

The satellite selection in this paper is based on the data of Deli-NEXT satellite by Delfi university, Netherland.

Table 1 Mission Data of Nano Satellite.

I_{xx}	I_{yy}	I_{zz}
0.0068138	0.0068138	0.001085

Table 2 Physical Properties of Nano Satellite (All in Kgm2).

Outer Dimensions	100×100×340 mm^3
Main Material	Aluminum
Total Mass	651g
Reference system	Geocentric
Regime	Low Earth Orbit
Perigee	599km
Apogee	780km
Inclination	97.76
Orbital period	98.41 minutes

III. ENVIRONMENTAL PERTURBATIONS

Even in space, there are natural forces that in turn make bodies tumble. These forces are caused by solar radiation, gravity gradient, Earth magnetic field and aerodynamics.

1. Aerodynamic Torque

Aerodynamic forces in near Earth orbit leads to drag and reduces the altitude over time. These forces that act on the spacecraft body and is presented as [11].

$$T_a = \frac{1}{2}\rho C_d A_r V^2 (c_{P_a} - c_m) \quad (2)$$

where T_a is the atmospheric torque, ρ is the atmospheric density in kg/cm^3, C_d is the drag coefficient (usually between 2 and 2.5 for spacecraft), A_r is the ram area in m^2, V is the spacecraft's orbital velocity in m/s, and c_{pa}-c_m is distance between centroid and center of mass. The result of aerodynamic torque is expressed in Table 3.

Table 3 Aerodynamic Torque Calculation

Atmospheric density	ρ	1.67× $10^{-13} kg/m^3$
Ram area	A_r	100mm×340mm
Spacecraft's orbital velocity	V	7.558 km/s
Distance between Centroid and center of mass of spacecraft	c_{P_a} -c_m	0.0005 m
Drag coefficient	C_d	2
Atmospheric torque	T_a	1.33× 10^{-9} N-m

2.Gravity Gradient Torque

A spacecraft in low orbitdoes not experience the same gravitational pull on allparts of its body, which causes the spacecraft to turntowards the Earth in accordance

with the principal axisof inertia. According to [11] the torque is expressedas

$$T_g = \frac{3\mu}{2R}|I_z - I_y|\sin(2\theta) \quad (3)$$

The result of gravity gradient toque is expressed in Table 4.

Table4 Calculation of Gravity Gradient Torque.

Earth's gravitational constant	μ	$3.986\times 10^{14}m^3/s^2$
Distance from the center of the Earth	R	6977 km
Moment of inertia about Z	I_z	0.0010835 $kg.m^2$
Moment of inertia about Y	I_y	0.0068138 $kg.m^2$
Angle between the local vertical and the Z principal axis	θ	2 degree
Gravity gradient torque	T_g	3.519×10^{-10} Nm

3. Solar Radiation Torque

The torque produced whenradiation and particles from the Sun hits the satellitebody can be found as a scalar by [11]

$$T_s = \frac{\phi}{c} A_s (1+q)(c_{P_s} - c_m)\cos\beta$$

Solar radiation torque is calculated in Table 5

Table 5Calculation of Solar Radiation Torque.

Solar constant	∅	1366 W/m^2
Speed of light	C	3×10^8 m/s
Sunlit surface area	A_s	100mm×100mm
Reflectance factor	q	0.6
Angle of incidence of the sun	□	0 deg
Distance between Centroid and center of mass of spacecraft	c_{P_s} -c_m	0.01m
Solar radiation pressure torque	T_s	7.28×10^{-10} N-m

5. Magnetic Field

Type your main text in 10-point Times, single-spaced. Do notuse double-spacing. Your paper must be in two column format with a space of 0.2" between columns. Be sure your text is fully justified—that is, flush left and flush right. Please do not place any additional blank lines between paragraphs.

The Earth's liquid core is a dynamo that generates a magnetic field powerful enough to have important effects on the space surrounding the planet. Most spacecraft have some level of residual magnetic moment, meaning they have a weak magnetic field of their own. These residual moments can range anywhere from 0.1-20 $A.m^2$, or even more depending on the spacecraft's size and whether any onboard compensation is provided.

When a spacecraft's residual moment is not aligned with a local magnetic field, it experiences a magnetic torque that attempts to align the magnet to the local field, much like a compass needle. The Earth's magnetic field is complex, asymmetric, not aligned with the Earth's spin axis, and varies with both geographical movement of the dipole and changes in solar particle flux. However, the maximum toque experienced by satellite is expressed as [11].

$$T_m = DB = D\left(\frac{M}{R^3}\lambda\right) \quad (5)$$

The result of magnetic torque is expressed in Table 6.

Table 6 Calculation of Magnetic Torque

Residual dipole moment	D	0.4 $A.m^2$
Magnetic constant	M	$7.8\times 10^{15}Tm^3$
Spacecraft altitude	R	6378+599 km
magnetic latitude	λ	2
Magnetic torque	T_m	1.837×10^{-5} N-m

From all external perturbation torque calculation, the maximum torque of satellite experienced in orbit is about 1.837×10^{-5} N-m.

IV. FLYWHEEL DESIGN

Flywheel is a device which stores a large amount of angular momentum and applying conservation of angular momentum law in the satellite and simulator to control attitude [4].

1. Flywheel Design for Satellite

A simple disk-shaped flywheel is designed for the Nano satellite reaction wheel system. A simple design was chosen to minimize the risk of unbalance in the manufactured flywheel caused by manufacturing imperfections. Fig. 2 shows a design of the flywheel accompanied by its 3D model.

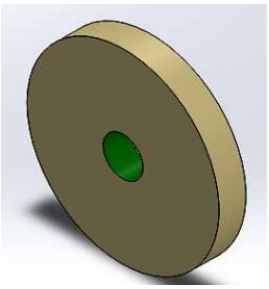

Fig.2 Flywheel design for satellite.

Each reaction wheel needs to store angular momentum over a dynamic range of 1.56×10^3 Nms. Since RWS includes flywheels and motor, Faulhaber 1202 004BH

as shown in Fig. 3 is chosen due to its high rotation speed range. Therefore, taking the moment of inertia of the motor itself into account, the flywheel moment of inertia around the axis of rotation must be at least [10]:

$$I_{zz} > \frac{30.H_{req}}{n_{max}\pi} - I_{motor} \quad (7)$$

Where I_{ZZ} is the required flywheel moment of inertia ($kg.m^2$), n_{max} is the maximum useful speed (rpm). H_{req}equals half the required dynamic range (N-m-s) and I_{motor} is the rotor moment of inertia. For the Faulhaber 1202 004 BH is 1.25×10^{-8} $kg.m^2$ from motor specification sheet. The maximum useful speed was 29,300 rpm for motor. To account for design uncertainties in the preliminary design phase, a margin of 10% is taken on the maximum useful speed and the flywheel is designed for a maximum useful speed of 26,370 rpm. Flywheel specification is expressed in Table4.

Fig.3 Faulhaber 1202 004BH motor [10].

1. Flywheel and Platform Design for Simulator

The motor for simulator is selected Emax CF 2805 motor as in Fig. 4 and its moment of inertia is 5.0123×10^{-7} $kg.m^2$. The platform design is based on the motor and the material is Aluminum due to its light weight and high resistance in vibration. The platform specification is described in Table VII and platform design used in simulator is as shown in Fig. 5.

Fig.4 Emax CF 2805 motor.

Table 7 Specification of Simulator Platform.

Material	Al	Aluminium
Size	-	20cm×20cm×0.2cm
Density	ρ	2.80 g/cm^3
Mass	m	224 g
Moment of inertia	I	$1.4933\times10^{-3}kgm^2$

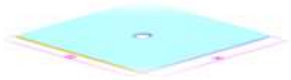

Fig.5 Platform design for simulator.

After designing the simulator design, the flywheel is constructed to install in the simulator for maintaining its attitude. The motor can rotate in both directions, therefore, $H=7.466\times10^{-4}$ N-m-s (half of total angular momentum). By using Equation (7), the moment of inertia required for flywheel is 2.28809×10^{-6} kgm^2. Bronze material is selected due to its durability and minimization in electromagnetic effects [10] as shown in Fig.6. The final platform of reaction wheel system is described in Fig.

Fig.6 Flywheel used in simulator.

Fig.7 Model of simulator

.

V. INTERNAL DISTURBANCE

The internal torques are also known as momentum exchange torques because they result in, or are result of the exchange of angular momentum between components of complex spacecraft without a change in the net system of the entire spacecraft. Some internal torques constitute undesirable disturbances, while others are provided by control mechanisms [6,13].

For internal disturbance analysis, some assumptions are made for the model. The spacecraft is a perfectly rigid body and has no normal vibrational modes. The configuration of reaction wheels is allocated as shown in Fig.8. These wheels are concentric, identical wheels, spatially aligned with the center of mass of mass location are assumed along the Z-axis [5,7].

Deviations of the wheels from the assumption of perfect balance made in are a principal contributor to disturbances. These deviations are classified as static imbalance or dynamic imbalance.Static imbalance is the

International Journal of Scientific Research & Engineering Trends
Volume 4, Issue 5, Sept-Oct-2018, ISSN (Online): 2395-566X

condition that the wheel's center of mass is not on the axis of rotation [8,9,13]. In this case, the spacecraft must provide, through the bearing assembly, the centripetal force needed to continuously accelerate the center of

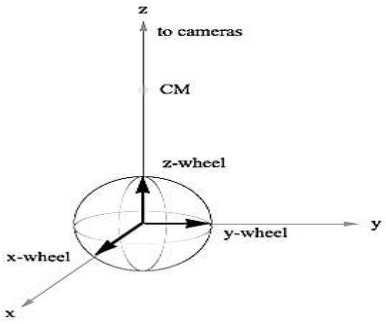

Fig.8 Simplified model of RWS [5].

mass in a circular motion about the axis of rotation. Dynamic imbalance is the condition that the axis of rotation of the wheel is not a principal axis. Static imbalance is only interested here.Static Imbalances are radial asymmetries in mass distribution. Each spinning wheel with a static imbalance impose a periodic force on the spacecraft. The magnitude of the force vector is constant however its direction changes with time. The set of all forces and torques on the body due to any static imbalance as a function of wheel angular velocities is as [5]

$$F_s(\omega_x,\omega_y,\omega_z)=(S_y\omega_y^2 sin(\omega_y t+j_y)+S_z\omega_z^2 cos(\omega_z t+j_z))\hat{x}$$
$$+(S_z\omega_z^2 sin(\omega_z t+j_z)+S_x\omega_x^2 cos(\omega_x t+j_x))\hat{y}$$
$$+(S_x\omega_x^2 sin(\omega_x t+j_x)+S_y\omega_y^2 cos(\omega_y t+j_y))\hat{z}$$

..(8)

As a result, any force not acting through the center of mass also acts as a torque on the spacecraft and described as [5].

$$\vec{\tau}_s(\omega_x,\omega_y,\omega_z)=\vec{R}_\omega\times\vec{F}(\omega_x,\omega_y,\omega_z) \quad (9)$$

Wheel static imbalance S_x, S_y, S_z is 7.947×10^{-13} kg.m^2 and $\omega_x, \omega_y, \omega_z$is rotation speed of wheel and their maximum speed is 29300 rpm at each axis. The j_x, j_y, $j_z$is for the pixel in the farthest corner of the camera-array's field of view, 45° off the Z-axis in the Y-direction and 27° off-axis in the X-direction.

The magnitude of periodic angular displacement calculated from Equation (8) and (9) is interested in this section. Fig.9 shows the expected jitter in terms of angular displacements as a function of time for the case of two wheels (Y and Z) running at the same speed (29300 RPM) while the third is still.

Fig.10 also shows the expected jitter in terms of angular displacement as a function of time for the case of three wheels (X, Y, Z) running at the differential speed (29300 RPM,20000 RPM,10000 RPM). The model shows a maximum angular error less than 10– 7 radians = 0.2 arcseconds [5] and it is safe for system. The internal torque can be neglected for the system as showing from the result.

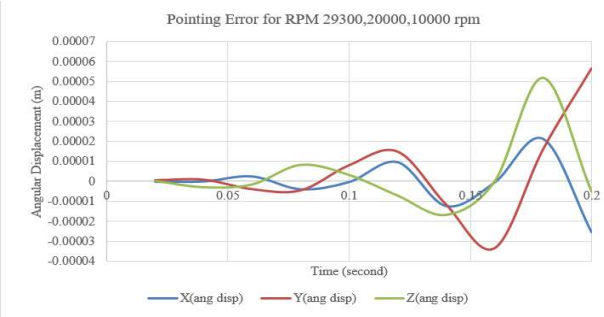

Fig.9. Jitter profile for X-wheel: 0 RPM, Y-wheel: 29300 RPM, Z-wheel: 29300 RPM

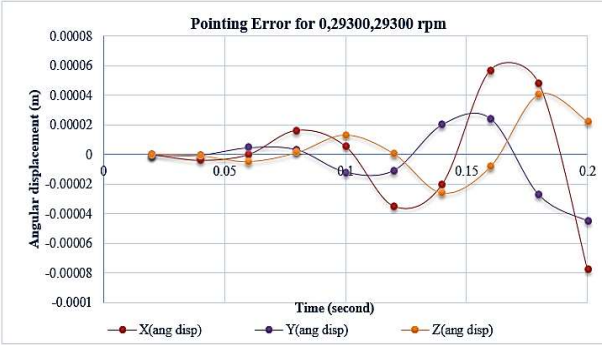

Fig.10 Jitter profile for X-wheel: 293000 RPM, Y-heel: 29300 RPM, Z-Wheel 29300 RPM

VI. SYSTEM MODELLING

There are two governing equations for BLDC motor, namely Newton's Second law of motion and Kirchhoff's Voltage law. Newton's Second law of motion states that

$$I\,\dot{\omega} = \sum M \quad \text{.....(10)}$$

Where Iis the moment of inertia [kg.m^2], □ is the rotation speed [rad/s] and $\sum M_0$ is the sum of all moments around the body's centre of gravity. Kirchhoff's Voltage Law dictates that

$$U=RI+L\frac{dI}{dt} \quad \text{.....(11)}$$

Where U is the voltage that applied over the motor [V], R is the motor terminal resistance [□], I is the current [A] and L is the terminal inductance from phase to phase.

For a brushless DC motor, $\sum M_0$is expressed by:

$$\sum M_0=k_m I-(C_0+C_v\times n) \quad \text{.....(12)}$$

Where k_m is the motor torque constant [Nm/A], C_0 is the motor static friction [Nm] and C_v is the motor dynamic friction coefficient [Nm/rpm]. C_v includes viscous

fiction of the ball bearing as well as Foucault currents in the stator caused by rotating magnetic field of the magnet. From above equation

$$\frac{\pi I}{30}\dot{n} = k_m I - (C_0 + C_v \times n) \quad \text{.....(13)}$$

Where n is the rotation speed [rpm]. The next step is to get rid of *I* because it cannot be measured or directly control. By adding the motor back-EMF constant k_E [V/rpm].

$$U = R I + L \frac{dI}{dt} + k_E n \quad \text{.....(14)}$$

Express *I* as the function of other variables:

$$I = \frac{U}{R} - \frac{k_E}{R} n - \frac{L}{R}\frac{dI}{dt} \quad \text{.....(15)}$$

Substitute *I* in equation:

$$\frac{\pi I}{30}\dot{n} = k_m \left(\frac{U}{R} - \frac{k_E}{R} n - \frac{L}{R}\frac{dI}{dt}\right) - (C_0 + C_v \times n) \quad \text{...(16) 13}$$

In which I is substituted by

$$\frac{dI}{dt} = -\frac{\dot{n} k_E}{R} \quad \text{.....(17)}$$

Finally, equation of motion describing mathematical representation is derived as follows

$$\dot{n} = \frac{30 k_m k_E R + 30 C_v R^2}{30 L k_E k_m - \pi I R^2} n + \frac{30 k_M R}{\pi I R^2 - 30 L k_E k_m} U + \frac{30 R^2 C_0}{30 L k_E k_m - \pi I R^2}$$

The full system is now describing with only n and U as variables, where n is the state variable and U is the control variable.Alternatively, this equation is rewritten as:

$$\left(\frac{\pi I R}{30 k_m} - \frac{L k_E}{R}\right)\dot{n} + \left(k_E + \frac{C_v R}{k_m}\right) n = U - \frac{R C_0}{k_m} \quad \text{.....(19)}$$

By taking Laplace transform on above equation, the resulted equation is

$$\left[\left(\frac{\pi I R}{30 k_m} - \frac{L k_E}{R}\right) s + k_E + \frac{C_v R}{k_m}\right] N(s) = \left[U - \frac{R C_0}{k_m}\right] W(s) \quad \text{.....(20)}$$

Where W(s) is a step function. The transfer function is then:

$$G(s) = \frac{N(s)}{W(s)} = \frac{U - \frac{R C_0}{k_m}}{\left(\frac{\pi I R}{30 k_m} - \frac{L k_E}{R}\right) s + k_E + \frac{C_v R}{k_m}} \quad \text{....(21)}$$

VII. CONTROLLER DESIGN

The control system is required to adjust the output result with the desired input. Firstly, open loop control is tested to the system. The reaction wheels are operated at3.5 Volt. The values of U=3.5V, C_0= 0.003 10-3 and R=16 is inputted to above equation and the resulted transfer function is

$$G(s) = \frac{3.25}{0.0005479\ s + 0.000103}$$

The step is fed to the system with the open loop control,

The resulting response curve is as shown in Fig.11.The result shows that the rise time take about 11.7 seconds where rise time is the time taken by a signal to change from a specified low value to a specified high value. It is analog parameter of fundamental importance in high speed electronics, since it is a measure of ability of a circuit to respond to fast input signals. It is also shown that maximum rotation speed (29300 rpm) of the motor is not enough to get the stable system of the satellite when the disturbance torques are experienced. Therefore, closed system is considered for the system to reduce errors and improve stability.

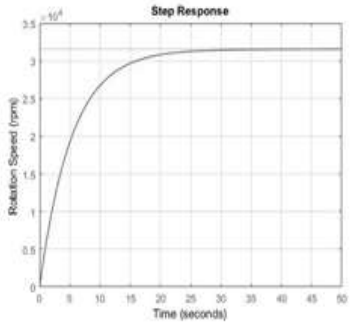

Fig.11.Simulated open loop reaction wheel response.

1.P- Controller

P- controller is the simplest feedback controller is one for which the controller output is proportional to error signal It has the disadvantage that there may be a steady-state error [14]. The transfer function for Proportional control is

$$G(s) = \frac{0.0001399}{0.0005479\ s + 0.0002429}$$

The response of P-controller is shown in Fig.12. The rise time is reduced to 5 second from 11.7 second but the steady state error is huge for the system. The steady state can reach only 0.576 instead of stable 1. Therefore, P-controller is not compatible for our system.

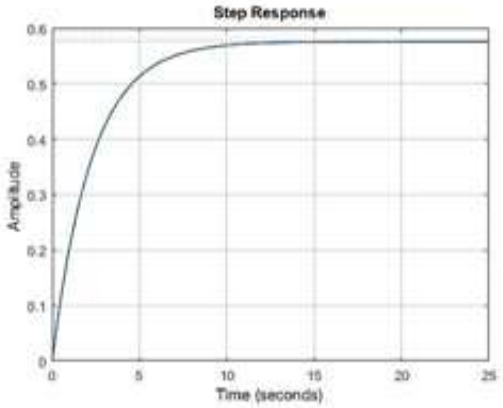

Fig.12 Response of the system with P-controller.

Table 8 Gains for P, PI, PID Controllers..

Controller	$K_p(\times 10^{-5})$	K_i	$K_d(\times 10^{-5})$
P-controller	4.305		
PI-controller	3.8745	5.1936×10^{-6}	
PID-controller	5.166	1.1495×10^{-5}	5.804

2.PI- Controller

The steady-state error can be eliminated by using an integral controller. The advantage of the integral controller is that the output is proportional to the accumulated error. The disadvantage of the integral controller is that we make the system less stable by adding the pole at the origin [14]. By combing of proportional and integrative gain, the transfer function of PI controller is

$$G(s)=\frac{0.0001399\ s + 1.688e\text{-}05}{0.0005479s^2+0.0002429s+1.688e\text{-}05}$$

The system gives the response as in Fig. 13 with the rising time of 15.2 second. It takes more time to rise while it is comparing with P-controller but it eliminates the steady error.

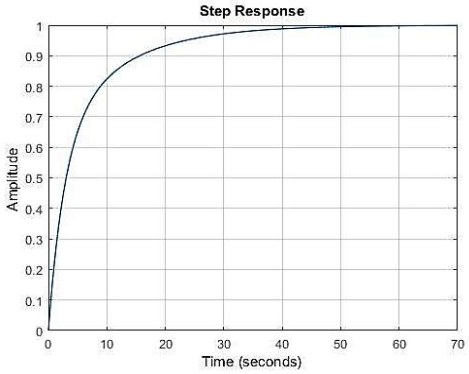

Fig.13 Response of the system with PI controller.

3.PID- Controller

The advantage of the derivative controller is that the controller will provide large correction before the error becomes large. The major disadvantage of the derivative controller is that it will not produce a control output if the error is constant. Another difficulty on the derivative controller is its susceptibility to noise. The derivative controller in its present form would have difficulty with noise problems. Each of the controllers-providing proportional, integral, and derivative control-has it advantages and disadvantages. The disadvantages of each controller can be eliminated by combining of three controllers into a single PID controller [14]. The continuous transfer function with PID controller is

$$G(s)=\frac{0.0001886s^2+0.0001399s+1.688e-05}{0.0007365s^2+0.0002429s+1.688e-05}$$

The resulted curve is described in Fig.14. The rise time is increased to 18.8 seconds in this controller and 35.4 second is required for settling time of the system. It eliminates steady state error of system.

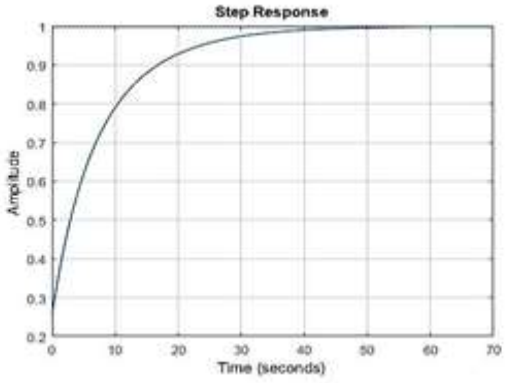

Fig.14 Response curve of the system with the PID controller.

The controllers and their response curves are described above all. From that, P-controller is not compatible with the system although the rise time is fast, the steady state error is not qualified. PI and PID controllers can be used for our system to fulfil the mission requirements.

VIII. CONCLUSION

In order to improve the pointing capabilities of Nanosat, a fast and precise response control system is required. Reaction wheels are an effective solution and rely on the simple principle of conservation of angular momentum. The project is intended to design, verify the Reaction Wheel System (RWS) for Nano satellite in space environment and construct the model which shows the function of RWS by controlling the attitude of its platform.

The calculation of the perturbation torques that should be applied enabled to determine the maximum torque expected to be delivered by the RWS during its orbital movement. This has allowed to define the upper bound for the expected torque to be delivered.

In flywheel design, it was calculated based on the angular momentum required of system and its resistivity on the harsh space environment. An extensive analysis of the torques caused by the internal disturbances, static imbalance is also calculated and proved to have a negligible effect on the satellite reliability. The analysis based on MATLAB and a Simulink model confirmed the viability of the system. It has been shown that a good and fast response for the desired input torques to be provided by each wheel is achievable. Moreover, the rotation time of reaction wheel system is identified to get the desired position of state from undesirable mode.

In controller design, although the wheel speed is over its maximum speed, the system is not stable in open loop system. The rising time is enough but the steady state error is huge in P-controller. The steady state error is eliminated in PI and PID controller and the rising time is compatible for the system. PID have complex system when comparing with PI-controller.

ACKNOWLEDGMENT

The author would like to acknowledge Space Systems Department. And also like to thank PhyoWai Thaw and Zin Win Thu for many insightful conversations and comments as well as for helping research works. The author expresses appreciation for the criticism of the referees, as a way of improving this paper.

REFERENCES

[1] E. Buchen and D. DePasquale. "Nano and Microsatellite Market Assessment Reaction Wheel System for CubeSat applications". SpaceWorksEnterprises, Inc., 2014
[2] Ricardo Filipe Pereira Gomes" Development of a reliable and low cost miniaturized,"M.Eng.thesis, April, 2018
[3] .Edited by James R. Wertz, Spacecraft Attitude Determination and Control. (Reprinted at 2002)
[4] Bhanu Gouda, Brian Fast, Dan Simon, Satellite Attitude Control System Design Using Reaction Wheels. (2004)
[5] Lulu Liu, Jitter and Basic Requirement for Reaction Wheel Assembly in the Attitude Controll Sysytem, (200
[6] Shahin S. Nudehi, Umar Farooq, Aria Alasty and Jimmy Issa, Satellite Attitude Control Using Reaction Wheels". (2008)
[7] Jeffery J Logan, Control and Sensor Development on a Four Wheel Pyramidal Reaction Wheel Platform. (2008)
[8] Espen Oland and Rune Schlash, Reaction wheel design for cubesats. (2009)
[9] Ryan E. Snider, Attitude Control of a Satellite Simulator Using Reaction Wheels and a PID Controller. (2010)
[10] Daegyun Choi, Dong Ik Cheon, Eunjeong Jang and Hwa-Suk Oh, Disturbance reduction on the small satellite actuator, (2011)
[11] Wertz, Everett & Puschell (eds.), Space Misssion Engineering:The New SMAD,(2011)
[12] G.L. Hoevenaars, Design Integration and Verification of the Delfi-n3Xt Reaction Wheel System. (2012)
[13] F.Landis Markley and John L. Crassidis, Fundamentals of Spacecraft Attitude Determination and Control, Springer.(2014)
[14] Courtland D. Perkins, Robert E. Hage, "Airplane Performance, Stability and Control". 1st edition, Jan 15,1949